AIAA AVIATION Forum
12-16 June 2023, San Diego, CA and Online
AIAA AVIATION 2023 Forum

10.2514/6.2023-4295

Direct noise predictions of a 360° fan stage using LES

J. Al Am* and V. Clair, A. Giauque, J. Boudet,
Univ Lyon, École Centrale de Lyon, INSA Lyon, Université Claude Bernard Lyon I, CNRS, Laboratoire de Mécanique des Fluides et d'Acoustique, UMR 5509, 36 Avenue Guy de Collongue, F-69134, Ecully, France

F. Gea-Aguilera †
Safran Aircraft Engines, 77550 Moissy-Cramayel, France

In the present study, the broadband noise of an ultra high bypass ratio fan/OGV stage, developed at École Centrale de Lyon, is studied numerically. Wall-modeled large eddy simulations (LES) over a 360° full fan stage are performed for the first time, at approach conditions. The noise emissions in the fan stage are directly obtained by the fully compressible LES, using a well refined unstructured grid. Additionally, a LES over a periodic sector of the fan stage is performed using the same configuration and numerical setup as for the 360° LES. The results of the 360° and the periodic sector configurations are compared in terms of mean and turbulent flow parameters and acoustic pressure spectra. The impact of the periodic boundary conditions, usually used for high-fidelity simulations of turbofan engines, is thus assessed. A slightly lower pressure difference between the pressure and suction sides of the blade is obtained in the 360° LES in the blade tip region. The acoustic azimuthal decomposition, which can only be estimated using the 360° LES configuration, is presented. The evolution of the coherence function in the azimuthal direction is also studied, particularly between monitor points located in separate blade channels. The coherence functions in the radial and azimuthal directions between monitor points located in the same blade channel are compared between the 360° and the periodic sector configurations. Lower coherence levels are obtained in the 360° LES mainly at low and mid frequencies.

I. Introduction

To comply with new restrictive regulations, aero-engine manufacturers aim to optimize turbofan engines to improve efficiency and reduce pollutant and noise emissions. To fulfill these requirements, modern and future generations of aero-engines, such as ultra high by-pass ratio (UHBR) turbofan engines, present an increased by-pass ratio and a large fan diameter. For such turbofan engines, the fan-outlet guide vane (OGV) stage is one of the main noise contributors [1, 2]. The fan-OGV stage noise is usually characterized by tonal and broadband components. Tonal noise mainly arises from periodic interactions in the fan stage and directly depends on the blades and vanes counts. The fan stage tonal noise is well addressed in the literature. Many solutions have been proposed to reduce tonal noise, such as the implementation of acoustic liners in the inlet and exhaust ducts and the optimization of the blade count to take advantage of duct filtering [3]. The broadband noise arises from different stochastic mechanisms in the fan stage and is less documented in the literature. The main broadband noise mechanisms in a fan stage are the blade tip-leakage vortex noise, the trailing edge noise and the rotor-stator interaction noise. The blade tip-leakage vortex noise is generated by the interaction of the highly unsteady flow that develops from the gap between the tip of the fan blades and the outer casing with the trailing edge corner and the neighboring blades [**?**]. The trailing-edge noise results from the diffraction of the turbulent boundary layers at the trailing edges of the rotor blades and stator vanes. The rotor-stator interaction noise is generated by the interaction of turbulence in the rotor wakes with the leading edges of the stator vanes. This interaction generates an unsteady loading on the vanes. Over the past few decades, several techniques have been developed to model and predict broadband noise mechanisms in a fan stage [2, 4].

High fidelity simulations, such as large eddy simulation (LES) and direct numerical simulation (DNS), can nowadays be applied for turbomachinery applications, due to the recent progress in computing resources. These numerical simulations allow for a detailed description of the turbulent structures that produce broadband noise. Due to its prohibitive cost, DNS is still limited to academic configurations with small Reynolds numbers. In the current study, LES is considered to model both the complex turbulent flow and the noise emissions in the fan stage with high accuracy and

*PhD candidate, Ecole Centrale de Lyon, LMFA, jean.al-am@ec-lyon.fr.
†R&D Acoustics Engineer, Aerodynamics and Acoustics Department, fernando.gea-aguilera@safrangroup.com.

acceptable computational cost. The direct noise predictions from the LES are also compared to analytical models from the literature. The input data for these models are extracted from the LES. Hanson's [5] and Posson's [6, 7] analytical models are used to model the rotor-stator interaction noise, whereas Amiet's [8, 9] model is used for the trailing edge noise.

In order to reduce the computational cost, a periodic sector is usually considered in previous studies in the literature to analyze the broadband noise from a fan-OGV stage [10**?** –12]. The numerical simulation is usually coupled with an analytical model [14–16] or an acoustic analogy [10, 11], such as the Ffowcs Williams and Hawkings [19] analogy to compute the acoustic field. Fairly good agreement was found between the noise predictions using these approaches and the experimental data. The analytical approach, informed by numerical data, usually underestimates the noise levels, whereas the hybrid approach based on an acoustic analogy is known to overestimate the noise levels [11]. For fully compressible LES, the acoustic power can also be directly computed upstream and downstream of the fan stage. Good agreement was obtained between direct noise predictions from a periodic fan/OGV stage and analytical models [12]. To further reduce the computation cost, some studies use simplified configurations of the periodic sector, such as linear cascades [21] or radial slices [22].

For all the studies mentioned previously, the impact of periodic boundary conditions on the flow field and noise emissions is not investigated. Indeed, if periodic boundary conditions are used on the azimuthal boundaries, a perfect correlation is imposed between these boundaries. This may lead to an over-prediction of the correlation levels, mainly at low to mid frequencies. Furthermore, the distribution of the acoustic energy over the different acoustic duct modes is influenced by the periodic boundary conditions. Only the cut-on azimuthal acoustic modes that correspond to the periodic angular sector are allowed to propagate in the fan stage. Finally, to allow the use of periodic boundary conditions, the geometry is usually modified to ensure adequate blade and vane counts. Several techniques have been developed to ensure that the fan stage performance and the flow field are similar between the original and the modified configurations [23]. However, this geometrical modification is expected to have an impact on the noise emissions, particularly on the rotor-stator interaction noise.

In the present study, the flow field and the acoustic emissions from a fan-OGV stage are analyzed using a 360° LES. The numerical setup is carefully designed to ensure an adequate description of the turbulent structures in the boundary layers and the wakes and a proper propagation of the acoustic waves in the fan stage. The objectives of the present study are to investigate the influence of periodic boundary conditions on the flow field and noise emissions and to compute the full acoustic modal content upstream and downstream of the fan stage, directly from the LES. The 360° LES is compared to a periodic sector LES, which was performed in a previous work by the authors [12] using the same configuration and numerical setup.

The paper is organized as follows. Section II shows the configuration and the numerical setup used for the LES. Preliminary results are presented in Section III.

II. Numerical setup

A. Computational domain

The configuration used in the present study is the ECL5 fan/OGV stage, which has been designed at Ecole Centrale de Lyon [24, 25] using technical requirements for a mid-range commercial aircraft. The ECL5 fan stage is a new open test case, which corresponds to an UHBR aero-engine with a low rotational speed, without core flow. The ECL5 fan stage is composed of 16 fan blades and 31 OGVs.

The computational domains of the 360° and periodic sector configurations are presented in Figure 1. The same angular extent for the rotor and stator domains is required by the AVBP solver [26]. Consequently, only for the periodic sector, the original configuration of 31 OGVs is adapted to 32 OGVs to allow for a $2\pi/16$ angular periodicity. In this case, the chord length is adjusted in a way that maintains the same solidity of the OGV, which is defined as the ratio between the chord length and the inter-vane spacing. This allows to maintain the stage performance [23]. The computational domain extends from 3.75 fan chord-lengths upstream of the rotor to 4.25 vane chord-lengths downstream of the stator. The distance upstream of the fan is chosen to ensure a well-developed boundary layer on the casing.

The present simulations are performed at approach conditions with a rotational speed of $\Omega = 6050$ rpm, which corresponds to 55% of the nominal rotational speed Ω_n.

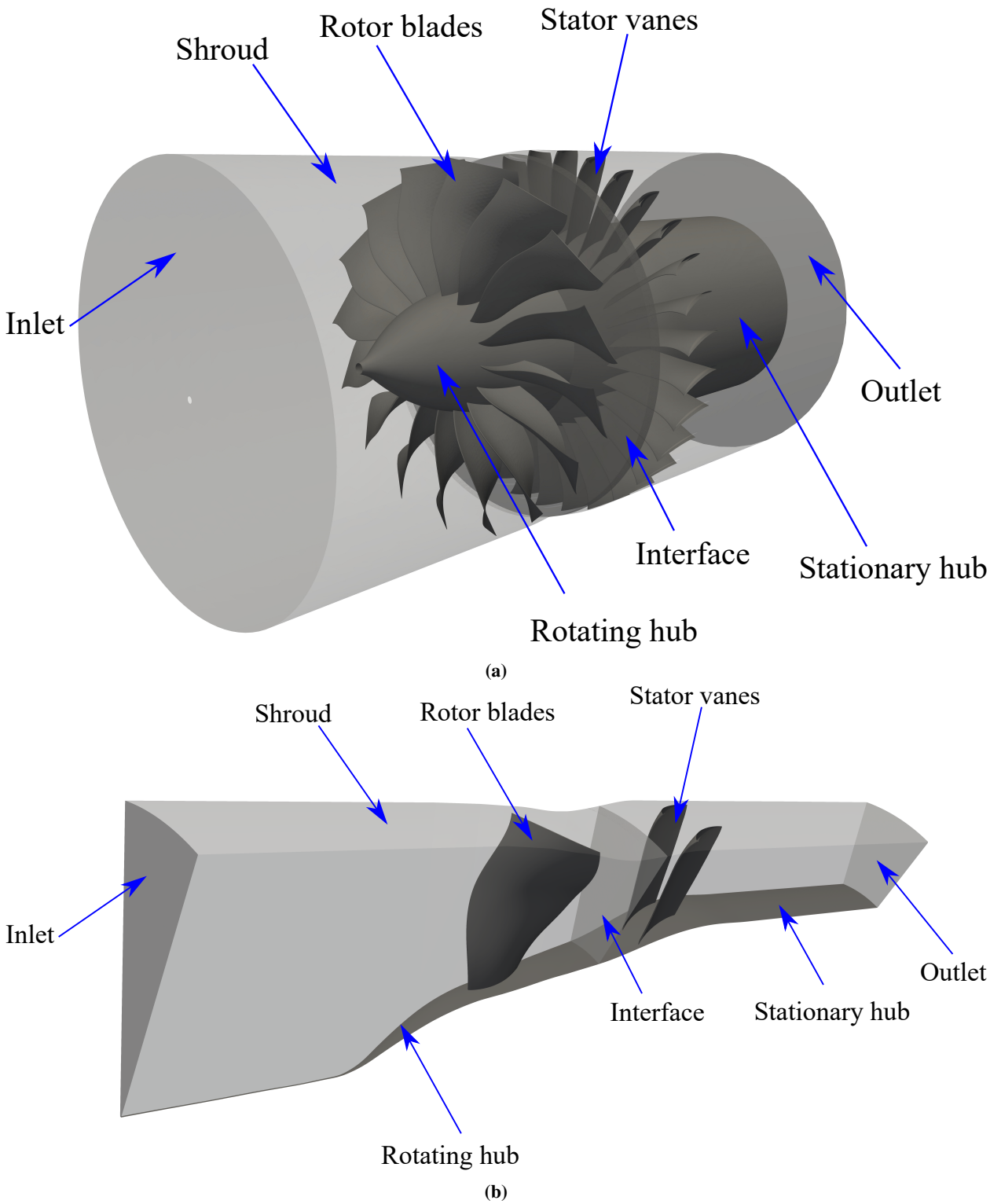

Fig. 1 Computational domains of (a) the 360° and (b) the periodic sector ECL5 fan/OGV stage.

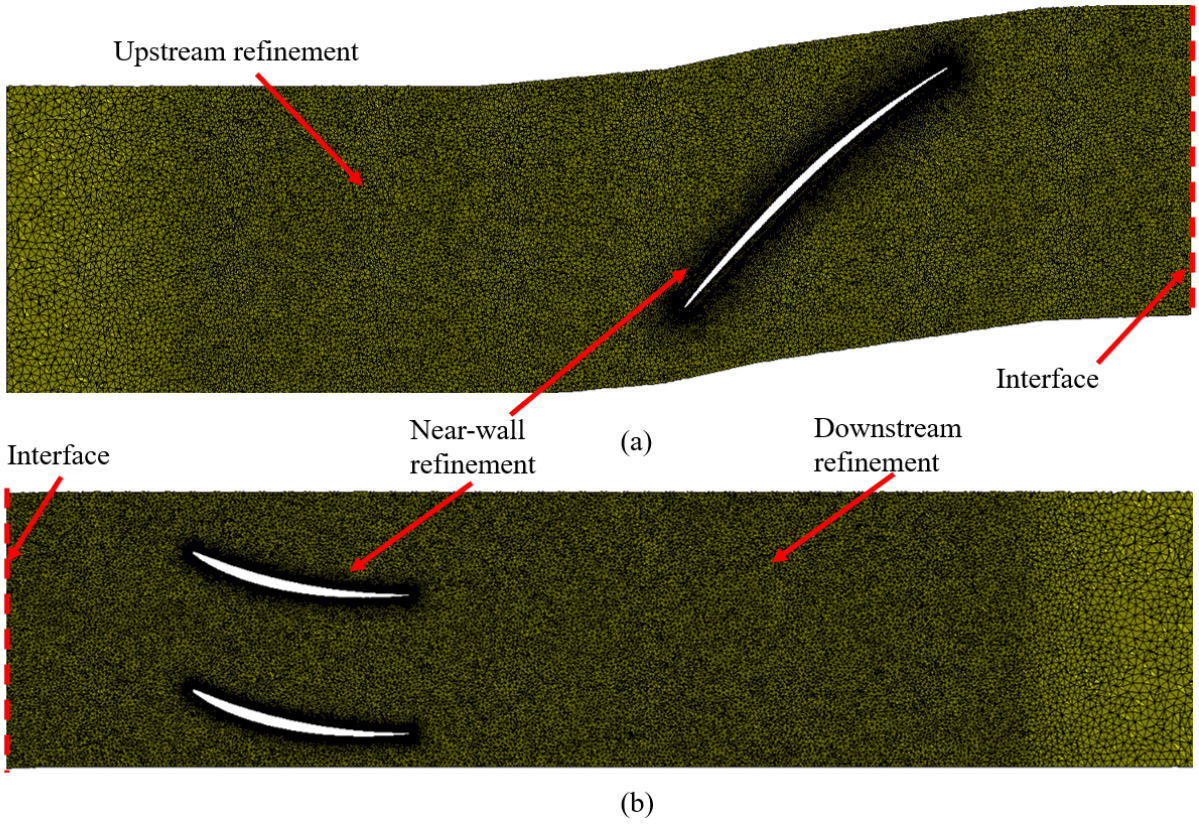

Fig. 2 Grid in a blade-to-blade view at 80% of the rotor span. (a) Mesh refinements in the rotor domain. (b) Mesh refinements in the stator domain.

B. LES numerical parameters

In the present study, the LES governing equations are solved using the AVBP solver [26]. AVBP is an explicit unstructured fully-compressible LES solver developed by CERFACS [26]. For the present turbomachinery application, two LES domains (rotor and stator domains) are coupled using the coupler CWIPI, which is based on an overlapping grid method [27]. The rotor domain contains the fan blades, and the stator domain contains the OGV.

The convective scheme used to solve the filtered Navier-Stokes equations is the two steps Taylor Galerkin (TTGC) [28] scheme, which is a third order finite-volume convective scheme. The unresolved turbulent eddies are modeled using the SIGMA sub-grid scale model [29]. At the inlet and outlet sections, non-reflecting Navier-Stokes Characteristic Boundary Conditions (NSCBC) [30] are used. A uniform mean flow is injected at the inlet section in the axial direction, with a total pressure of $P_0 = 101325$ Pa and a total temperature of $T_0 = 300$ K. To obtain the desired mass flow rate in the fan stage, the static pressure is adjusted at the outlet section. For the periodic sector, periodic boundary conditions are used on the azimuthal boundaries of the computational domain. On the wall surfaces of the blades, vanes, shroud and hub, a no-slip boundary condition is used. A wall law [31] is used to model the inner part of the boundary layer. A dimensionless velocity relative to the wall $u^+ = \frac{1}{\kappa}\ln(Ay^+)$ for $y^+ > 11.45$, with $\kappa = 0.41$ and $A = 9.2$, is adopted. Below $y^+ = 11.45$, a linear law is imposed.

The time step for the simulations is $\Delta t = 2.8 \times 10^{-8}$ s and the computational time is approximately 105×10^3 CPUh per rotation for the periodic sector and 1700×10^3 CPUh per rotation for the 360° configuration. About three full fan rotations are performed for the numerical and statistical convergence, and four additional fan rotations are expected for the post-processing and acoustic data collection in the final version of the paper.

C. Mesh characteristics

The grid at mid-span around the rotor blade and stator vanes is shown in Figure 2. The grid is an unstructured hybrid mesh composed of different types of elements: prismatic cells are used on the walls of the blades, vanes, shroud and

Table 1 Mesh properties of the LES grids. x^+, y^+ and z^+ are the maximum dimensionless wall distances in the streamwise, wall-normal and spanwise directions respectively.

	Sector LES	360° LES
Number of cells [10^6]	95	1500
x^+/z^+	150	150
y^+	25	25
Number of prism layers	10	10
expansion ratio	1.1	1.1
Time step [10^{-8}s]	2.8	2.8
CPUh/blade passage [10^3]	105	1700

hub, tetrahedral cells away from the walls, and pyramidal cells in the transition region between prismatic and tetrahedral cells. The mesh size and properties are chosen in a way to ensure a suitable resolution of the boundary layer and wake turbulence and to propagate the acoustic waves in the fan stage without significant dissipation and dispersion errors.

The main mesh properties for the periodic sector and 360° cases are given in Table 1. The near-wall refinement is based on predefined values of the dimensionless cell sizes, which are given by x^+, y^+ and z^+ in the streamwise, wall-normal and spanwise directions respectively. These distances are fixed below certain values, established in [32]. Close to the wall, the first prismatic layer has the smallest spacing. The cell size is then progressively increased using a chosen expansion ratio.

Away from the walls, the mesh density is based on both turbulent and acoustic criteria established by the authors in a previous work [32]. For the acoustic criterion, at least 13 points per wavelength ($\lambda_{ac} = \frac{c_0(1-M)}{f_c}$, where c_0 is the speed of sound, M is a mean Mach number, and $f_c = 20$ kHz is the desired mesh cut-off frequency) are used. This ensures a correct propagation of the acoustic waves up to a desired cut-off frequency.
For a proper description of the turbulent structures in the wake regions, the mesh size is smaller than 30 times the Taylor micro-scale ($\lambda_{Ta} = (10\frac{\nu k_t}{\epsilon})^{(1/2)}$, where ν is the kinematic viscosity, k_t the turbulent kinetic energy, and ϵ the turbulent dissipation rate). These two criteria directly depend on the numerical scheme and mesh topology and are found to provide accurate results in previous work [32].

III. Preliminary results

The 360° LES is still in progress and the sampling time used for the present results corresponds to one fan rotation. Thus, only preliminary results are discussed.

A. Instantaneous results

Figures 3 shows an isosurface of the Q-criterion ($Qc^2/U^2 = 10$) for the 360° LES configuration, along with contours of the instantaneous dilatation rate ($\nabla \cdot \mathbf{u}$) on a radial cut at 99% of the rotor span. The wave-fronts propagating in the upstream and downstream directions show the capability of the 360° LES to capture the noise propagation in the refined-mesh region around the fan stage. It should be noted that there is no visible acoustic reflection from the upstream and downstream boundaries of the domain. The iso-surface of the Q-criterion is colored by the vorticity magnitude. A qualitative description of the turbulent structures developing in the boundary layers and the wakes can be obtained. The transition of the boundary layers can be observed near the leading edges of the blades and vanes all along the span. Small turbulent structures can be seen downstream of the transition regions.

B. Mean quantities

Figure 4 shows a comparison of the distributions of isentropic Mach number, M_{is}, from the periodic sector LES and the 360° LES, along the rotor blade surface, for various spanwise positions. Similar results are obtained between the two configurations at 50% and 80% of the rotor span. A small recirculation bubble is associated to a flat region close to the leading edge on the suction side at 80% of the rotor span, and seems to be similarly captured by both configurations.

The spanwise position at 98% of the rotor span is much closer to the tip gap region and is affected by the tip-leakage

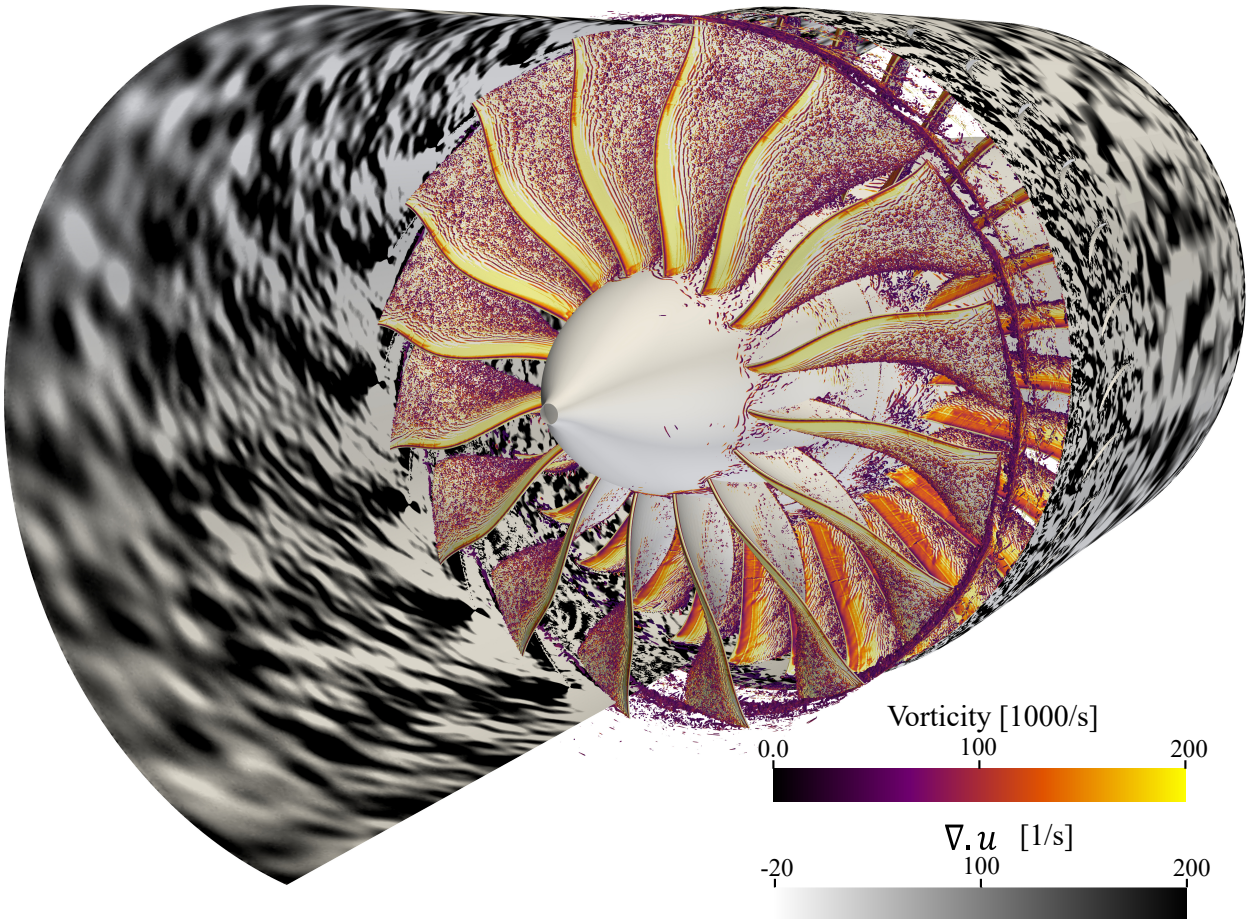

Fig. 3 Instantaneous contours of dilatation rate at 99% of the rotor span and iso-surface of Q-criterion ($Qc^2/U^2 = 10$) around of the rotor and the stator, colored by the vorticity magnitude, for the 360° LES configuration. View from an observer upstream of the fan looking at the suction side of the rotor blades.

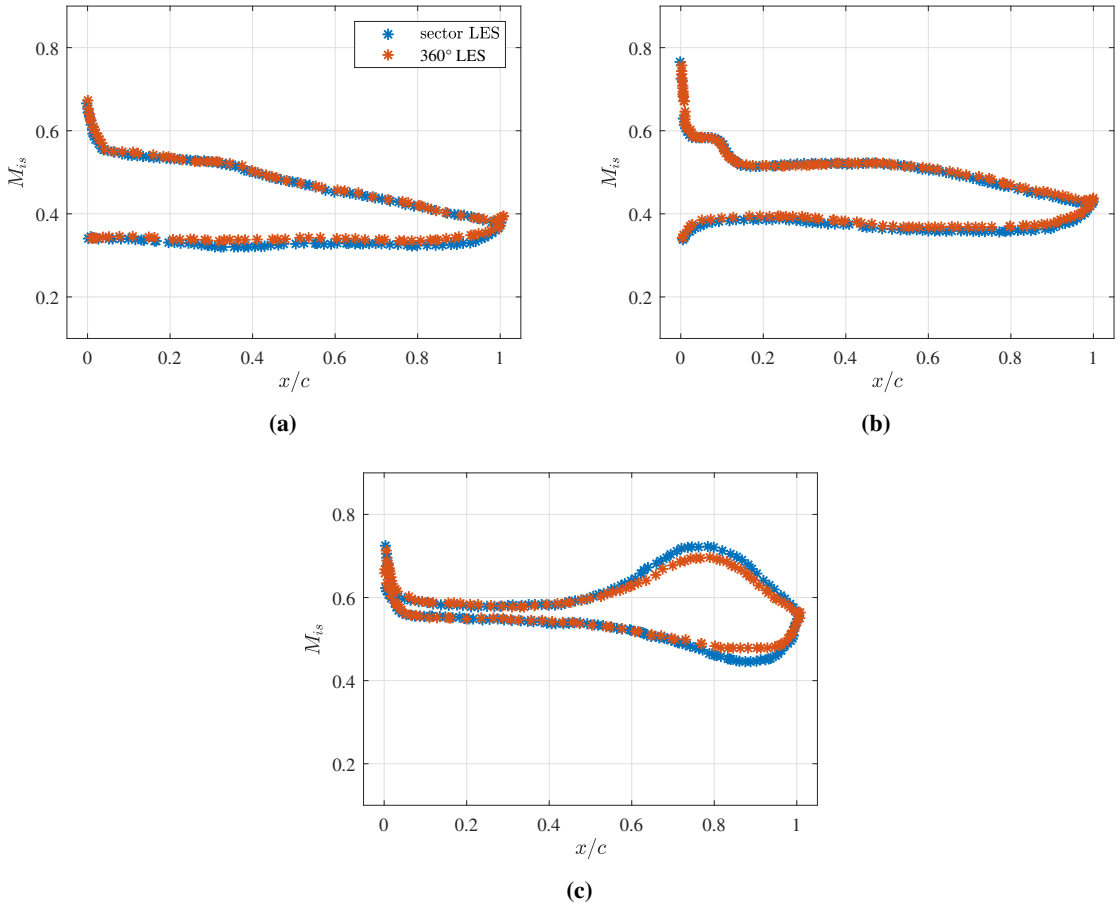

Fig. 4 Comparison between the periodic sector and the 360° LES, for the prediction of the average isentropic Mach number around the fan blade, at (a) 50%, (b) 80% and (c) 98% of the rotor span.

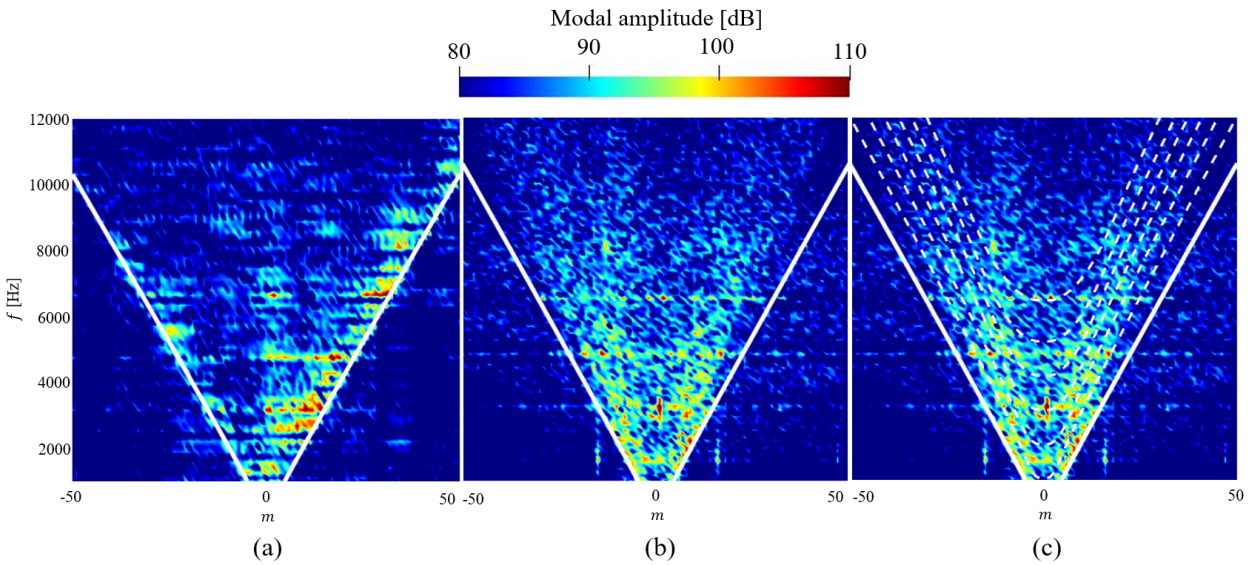

Fig. 5 Azimuthal mode detection plots at the (a) intake and (b,c) exhaust sections. The frequency is plotted against the azimuthal mode order m, and the modes are colored by their amplitude.

flow. The pressure difference between the leading edge and 40% of the chord length is similar for both configurations. Some differences between the two configurations are observed between 60% of the chord length and the trailing edge. For the periodic sector LES, a larger pressure difference between the suction side and the pressure side of the blade is observed in this region, compared to the 360° LES configuration. This suggests a difference in the tip flow topology, but may also be due to an insufficient statistical convergence of the 360° LES.

C. Modal decomposition

One of the main advantages of the 360° LES, compared to the periodic sector LES, is the ability to perform a complete azimuthal decomposition of the acoustic field radiated by the fan stage. However, at the time of redaction of this abstract, only one rotor rotation has been performed for the modal decomposition. Preliminary results are shown here and the analysis will only be qualitative. Quantitative results are expected subsequently for the final version of the paper.

The azimuthal modal contents at the intake and exhaust sections are presented in Figure 5, at 95% of the rotor span. 200 azimuthal monitor points located at one rotor chord length upstream of the rotor and one stator chord length downstream of the stator are used. The white solid line corresponds to the theoretical cut-off frequency of each azimuthal mode of order m for the first radial mode, $j = 0$, in an annular duct, and given by:

$$\omega_c = c_0 \beta K_{mj}, \tag{1}$$

where K_{mj} is the eigenvalue of the duct mode (m,j) and $\beta = \sqrt{1 - M^2}$ is the compressibility parameter. The white dashed lines correspond to the cut-off frequencies of the radial modes of orders ranging from $j = 1$ to $j = 6$.

Over the whole range of azimuthal modes, large modal amplitudes can be observed at the BPF and its harmonics. Moreover, the modal amplitudes are concentrated in the mode-frequency cut-on triangle, as expected (inside the V-shape delimited by the solid white lines). The cut-off modes are thus well attenuated, particularly at the exhaust section.

At the intake section (Figure 5 (a)), the modal content is seen to be slightly dominated by co-rotating modes ($m > 0$, which rotate in the same direction as the rotor). This co-rotating mode distribution was also observed experimentally on a fan stage at approach condition [33] and was related to the rotor-stator interaction noise source at the stator leading edge. This can be explained by observing the direction of the dipolar sources corresponding to the rotor-stator interaction noise, as shown in Figure 6. It can be seen that the dipole lobes of the rotor-stator interaction noise sources at the leading edges of the stator vanes are oriented in a way that will predominantly give rise to co-rotating acoustic modes.

Unlike the intake modal content, no clear trend towards the co-rotating or counter-rotating modes can be observed at the exhaust section in Figure 5 (b). It can be noticed that the slope of the actual V-shape containing the cut-on modes is

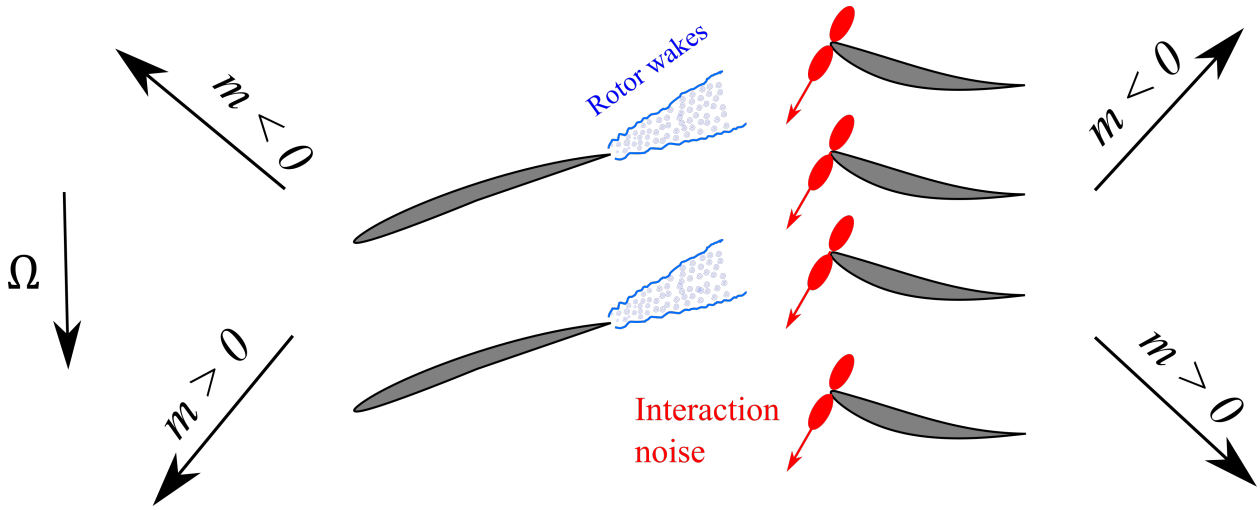

Fig. 6 A blade to blade schematic view of the fan/OGV stage illustrating the equivalent dipoles of the rotor-stator interaction noise on the leading edge of the stator vanes. The picture shows two rotor blades and four stator vanes. The direction of rotation is represented by the Ω arrow. The direction of co- and counter-rotating modes propagating upstream or downstream of the stage are also depicted.

slightly steeper than the theoretical cut-on/cut-off boundary represented by the solid white lines. For some azimuthal orders m, large amplitudes are visible at frequencies corresponding to the cut-on frequencies of the different radial modes (dashed lines in Figure 5 (c)). The azimuthal modes under the first dashed curve correspond to the first radial mode $j = 0$. At about 2 kHz, the radial mode $j = 1$ switches on, where large amplitudes can be observed. This behavior continues with more and more radial modes switching on.

IV. Conclusion

In the present study, the influence of the periodic boundary conditions on the flow topology and noise emissions of a fan stage has been investigated by comparing periodic sector and 360° LES configurations. The noise can be directly computed from the LES, by using a well refined mesh. The 360° LES is still in progress in order to obtain a fully-converged azimuthal modal decomposition.

The modal content of the ECL5 fan stage has been computed, by using the 360° LES. An azimuthal modal decomposition have been applied at 95% of the rotor span. Except for the first BPF at the exhaust section, the cut-off modes are sufficiently attenuated. At the different BPF harmonics, the Tyler and Sofrin's modes were clearly identified in the modal content, at both the intake and the exhaust section. At the intake section, a clear dominant co-rotating modal content is identified. At the exhaust section, a rippled structure is observed, where high modal amplitudes are observed at frequencies where additional radial modes become cut-on. This analysis is considered as the main advantage of a 360° LES compared to a periodic sector LES, for which the modal decomposition is limited by the azimuthal extent of the sector, whereas a complete azimuthal decomposition can be applied for the 360° LES.

The simulations are in progress. The more converged results will allow for a better understanding of the periodic boundary conditions limitations. Several aeroacoustic parameters, such as the radial profiles of the mean and fluctuating velocity components, the radial and azimuthal coherence functions, and the far field noise predictions, will be compared.

Acknowledgments

This work was performed within the framework of the industrial chair ARENA (ANR-18-CHIN-0004-01) co-financed by Safran Aircraft Engines and the French National Research Agency (ANR), and is also supported by the Labex CeLyA of the Université de Lyon, operated by the French National Research Agency (ANR-11-LABX-0060/ ANR-16-IDEX-0005).

The computational resources were provided by a PRACE European award (project LESFAN, proposal No. 2021240101), GENCI (CINES, project number A0082A05039), and by FLMSN-PMCS2I at Ecole Centrale de Lyon.

Most of the post-processing was performed using Antares (release 1.16.0, https://www.cerfacs.fr/antares).

References

[1] Envia, E., "Fan noise reduction: an overview," *International Journal of Aeroacoustics*, Vol. 1, No. 1, 2002, pp. 43–64. https://doi.org/10.1260/1475472021502668.

[2] Moreau, S., "Turbomachinery noise predictions: present and future," *Acoustics*, Vol. 1, No. 1, 2019, pp. 92–116. https://doi.org/10.3390/acoustics1010008.

[3] Tyler, J., and Sofrin, T., "Axial flow compressor noise studies," *Society of Automotive Engineers Transactions*, Vol. 70, 1962, pp. 309–332. https://doi.org/10.4271/620532.

[4] Moreau, S., and Roger, M., "Advanced noise modeling for future propulsion systems," *International Journal of Aeroacoustics*, Vol. 17, No. 6-8, 2018, pp. 576–599. https://doi.org/10.1177/1475472X18789005.

[5] Hanson, D. B., *Theory for broadband noise of rotor and stator cascades with inhomogeneous inflow turbulence including effects of lean and sweep*, National Aeronautics and Space Administration, Glenn Research Center, CR-2001-210762, 2001.

[6] Posson, H., Roger, M., and Moreau, S., "On a uniformly valid analytical rectilinear cascade response function," *Journal of Fluid Mechanics*, Vol. 663, 2010, p. 22–52. https://doi.org/10.1017/S0022112010003368.

[7] Posson, H., Moreau, S., and Roger, M., "On the use of a uniformly valid analytical cascade response function for fan broadband noise predictions," *Journal of Sound and Vibration*, Vol. 329, No. 18, 2010, pp. 3721–3743. https://doi.org/10.1016/j.jsv.2010.03.009.

[8] Amiet, R. K., "Noise due to turbulent flow past a trailing edge," *Journal of sound and vibration*, Vol. 47, No. 3, 1976, pp. 387–393. https://doi.org/10.1016/0022-460X(76)90948-2.

[9] Roger, M., and Moreau, S., "Back-scattering correction and further extensions of Amiet's trailing-edge noise model. Part 1: theory," *Journal of Sound and vibration*, Vol. 286, No. 3, 2005, pp. 477–506.

[10] Pérez Arroyo, C., Leonard, T., Sanjosé, M., Moreau, S., and Duchaine, F., "Large Eddy Simulation of a scale-model turbofan for fan noise source diagnostic," *Journal of Sound and Vibration*, Vol. 445, 2019, pp. 64–76. https://doi.org/10.1016/j.jsv.2019.01.005.

[11] Lewis, D., Moreau, S., Jacob, M. C., and Sanjosé, M., "ACAT1 fan stage broadband noise prediction using large-eddy simulation and analytical models," *AIAA Journal*, Vol. 60, No. 1, 2022, pp. 360–380. https://doi.org/10.2514/1.J060163.

[12] Al Am, J., Clair, V., Giauque, A., Boudet, J., and Gea-Aguilera, F., "Direct noise predictions of fan broadband noise using LES and analytical models," *28th AIAA/CEAS Aeroacoustics 2022 Conference*, 2022, p. 2882. https://doi.org/10.2514/6.2022-2882.

[13] Posson, H., Moreau, S., and Roger, M., "Broadband noise prediction of fan outlet guide vane using a cascade response function," *Journal of Sound and Vibration*, Vol. 330, No. 25, 2011, pp. 6153–6183. https://doi.org/10.1016/j.jsv.2011.07.040.

[14] Grace, S., Gonzalez-Martino, I., and Casalino, D., "Analysis of fan-stage gap-flow data to inform simulation of fan broadband noise," *Philosophical Transactions of the Royal Society A*, Vol. 377, No. 2159, 2019, p. 20190080. https://doi.org/10.1098/rsta.2019.0080.

[15] Grace, S. M., Gonzalez-Martino, I., and Casalino, D., "Analysis of fan-stage gap flow data generated using an LBM/VLES method," *25th AIAA/CEAS Aeroacoustics Conference*, 2019, p. 2668. https://doi.org/10.2514/6.2019-2668.

[16] Kissner, C., Guérin, S., Seeler, P., Billson, M., Chaitanya, P., Carrasco Laraña, P., de Laborderie, H., François, B., Lefarth, K., Lewis, D., Montero Villar, G., and Nodé-Langlois, T., "ACAT1 Benchmark of RANS-Informed Analytical Methods for Fan Broadband Noise Prediction—Part I—Influence of the RANS Simulation," *Acoustics*, Vol. 2, No. 3, 2020, pp. 539–578. https://doi.org/10.3390/acoustics2030029.

[17] Gonzalez-Martino, I., and Casalino, D., "Fan tonal and broadband noise simulations at transonic operating conditions using lattice-Boltzmann methods," *2018 AIAA/CEAS aeroacoustics conference*, 2018, p. 3919. https://doi.org/10.2514/6.2018-3919.

[18] Casalino, D., Hazir, A., and Mann, A., "Turbofan broadband noise prediction using the lattice Boltzmann method," *AIAA Journal*, Vol. 56, No. 2, 2018, pp. 609–628. https://doi.org/10.2514/1.J055674.

[19] Williams, J. F., and Hawkings, D. L., "Sound generation by turbulence and surfaces in arbitrary motion," *Philosophical Transactions for the Royal Society of London. Series A, Mathematical and Physical Sciences*, 1969, pp. 321–342. https://doi.org/10.1098/rsta.1969.0031.

[20] Goldstein, M., *Aeroacoustics*, Advanced book program, McGraw-Hill International Book Company, 1976. URL https://books.google.com.lb/books?id=HY1TAAAAMAAJ.

[21] Régis, K., Marlène, S., and Stéphane, M., "Aerodynamic investigation of a linear cascade with tip gap using large-eddy simulation," *Journal of the Global Power and Propulsion Society*, Vol. 5, 2021, pp. 39–49. https://doi.org/10.33737/jgpps/133601.

[22] Al-Am, J., Clair, V., Giauque, A., Boudet, J., and Gea-Aguilera, F., "On the effects of a separation bubble on fan noise," *Journal of Sound and Vibration*, Vol. 537, 2022. https://doi.org/10.1016/j.jsv.2022.117180.

[23] Rai, M. M., and Madavan, N. K., "Multi-Airfoil Navier–Stokes Simulations of Turbine Rotor–Stator Interaction," *Journal of Turbomachinery*, Vol. 112, No. 3, 1990, pp. 377–384. https://doi.org/10.1115/1.2927670.

[24] Brandstetter, C., Pagès, V., Duquesne, P., Ottavy, X., Ferrand, P., Aubert, S., and Blanc, L., "UHBR open-test-case fan ECL5/CATANA part 1: geometry and aerodynamic performance," *14th European Conference on Turbomachinery Fluid dynamics & Thermodynamics*, Gdansk, Poland, 2021.

[25] Pagès, V., Duquesne, P., Ottavy, X., Ferrand, P., Aubert, S., Blanc, L., and Brandstetter, C., "UHBR open-test-case fan ECL5/CATANA part 2: mechanical and aeroelastic stability analysis," *14th European Conference on Turbomachinery Fluid dynamics & Thermodynamics*, Gdansk, Poland, 2021.

[26] Schonfeld, T., and Rudgyard, M., "Steady and unsteady flow simulations using the hybrid flow solver AVBP," *AIAA Journal*, Vol. 37, No. 11, 1999, pp. 1378–1385. https://doi.org/10.2514/2.636.

[27] Wang, G., Duchaine, F., Papadogiannis, D., Duran, I., Moreau, S., and Gicquel, L. Y., "An overset grid method for large eddy simulation of turbomachinery stages," *Journal of Computational Physics*, Vol. 274, 2014, pp. 333–355. https://doi.org/10.1016/j.jcp.2014.06.006.

[28] Colin, O., and Rudgyard, M., "Development of high-order Taylor-Galerkin schemes for LES," *Journal of Computational Physics*, Vol. 162, No. 2, 2000, pp. 338–371. https://doi.org/10.1006/jcph.2000.6538.

[29] Nicoud, F., Toda, H. B., Cabrit, O., Bose, S., and Lee, J., "Using singular values to build a subgrid-scale model for large eddy simulations," *Physics of fluids*, Vol. 23, No. 8, 2011. https://doi.org/10.1063/1.3623274.

[30] Poinsot, T., and Lele, S., "Boundary conditions for direct simulations of compressible viscous flows," *Journal of Computational Physics*, Vol. 101, No. 1, 1992, pp. 104–129. https://doi.org/10.1016/0021-9991(92)90046-2.

[31] Schmitt, P., Poinsot, T., Schuermans, B., and Geigle, K. P., "Large-eddy simulation and experimental study of heat transfer, nitric oxide emissions and combustion instability in a swirled turbulent high-pressure burner," *Journal of Fluid Mechanics*, Vol. 570, 2007, pp. 17–46. https://doi.org/10.1017/S0022112006003156.

[32] Al-Am, J., Clair, V., Giauque, A., Boudet, J., and Gea-Aguilera, F., "A Parametric Study on the LES Numerical Setup to Investigate Fan/OGV Broadband Noise," *International Journal of Turbomachinery, Propulsion and Power*, Vol. 6, No. 2, 2021. https://doi.org/10.3390/ijtpp6020012.

[33] Pereira, A., and Jacob, M. C., "Modal analysis of in-duct fan broadband noise via an iterative Bayesian inverse approach," *Journal of Sound and Vibration*, Vol. 520, 2022. https://doi.org/https://doi.org/10.1016/j.jsv.2021.116633.